JOURNAL OF VIROLOGY, Aug. 2011, p. 7922–7927 Vol. 85, No. 15
0022-538X/11/$12.00 doi:10.1128/JVI.00834-11
Copyright © 2011, American Society for Microbiology. All Rights Reserved.

NOTES

Architecture and Regulation of the HIV-1 Assembly and Holding Compartment in Macrophages▽

Sonja Welsch,[1]* Fedde Groot,[2] Hans-Georg Kräusslich,[3] Oliver T. Keppler,[3] and Quentin J. Sattentau[2]

European Molecular Biology Laboratory, Meyerhofstrasse 1, D-69117 Heidelberg, Germany[1]; The Sir William Dunn School of Pathology, University of Oxford, South Parks Road, Oxford OX1 3RE, United Kingdom[2]; and Department of Infectious Diseases, Virology, University of Heidelberg, Im Neuenheimer Feld 324, D-69120 Heidelberg, Germany[3]

Received 23 April 2011/Accepted 11 May 2011

Productive infection of macrophages is central to HIV-1 pathogenesis. Newly formed virions bud into a tubular membranous compartment that is contiguous with the plasma membrane. However, little is known about the structure of this compartment and its potential regulation by infection. Here we characterized this compartment in macrophages using electron tomography and electron microscopy with stereology. We found an intricate, interconnected membrane network that constitutes a preexisting physiologic structure in macrophages but which expands in size upon HIV-1 infection. Membranes required for this expansion were apparently derived from preexisting pools of plasma membrane. Physical connections between this compartment and the extracellular milieu were frequently made by tube-like structures of insufficient diameter for virion passage. We conclude that HIV-1 induces the expansion of a complex membranous labyrinth in macrophages in which the virus buds and can be retained, with potential consequences for transmission and immune evasion.

Macrophages are important cellular targets of human immunodeficiency virus type 1 (HIV-1) (27). HIV-1-infected macrophages produce virus at a lower rate than $CD4^+$ T cells but remain viable for weeks or months as a result of HIV-1 suppression of apoptosis and are thus considered a viral reservoir (4, 18). Moreover, macrophages and microglia play important roles in HIV-1-related neurological disorders (10). Macrophage clearance of microorganisms that may become opportunistic pathogens in AIDS declines as macrophage function is impaired by HIV-1 infection, implying a central role for these cells in HIV-1 pathogenesis (17, 23).

HIV-1 replication in macrophages results in production of new virions that either may be released into the extracellular space or may be transmitted directly to other permissive cells via cell-cell contact (11, 13, 25). The major compartment into which HIV-1 buds has recently been described as an internally sequestered plasma membrane domain (3, 5, 19, 28). Although initially described as endosomal in nature (24), detailed analyses of infected macrophages labeled with the membrane-impermeant dye ruthenium red (RR) using electron microscopy (EM), and by ion abrasion scanning electron microscopy, have revealed virus-containing vesicular structures open to the exterior (2, 3, 5, 19, 28). These results are consistent with the idea that HIV-1 Gag preferentially buds from the plasma membrane (9, 16), although additional assembly of infectious HIV-1 into sealed endosomal compartments cannot be excluded (2, 14). Despite an increasing understanding of this compartment, questions remain regarding its three-dimensional (3D) topology, and it is unknown whether its morphology and/or size are altered upon HIV-1 infection. Using two-dimensional (2D) stereology and 3D electron tomography (ET) approaches, we analyzed the architecture of the HIV-1 assembly compartment and its morphological changes upon HIV-1 infection and reveal for the first time that macrophages contain a single or very few HIV-1 assembly compartments that expand upon HIV-1 infection.

Three-dimensional architecture of the HIV-1 assembly compartment. Primary monocyte-derived macrophage cultures were derived by a 6- to 8-day differentiation of peripheral blood monocytes by plastic adherence and cultivation in the presence of human AB serum, in principle as reported previously (28). CD14/CD68-positive macrophages were challenged with the Ba-L strain of HIV-1 ($HIV\text{-}1_{Ba\text{-}L}$), a CCR5-using macrophage-tropic virus, and 7 days postinfection, cells were fixed and stained with RR and embedded in plastic. Their ultrastructure was analyzed in single images from ultrathin sections and in tomograms from serial 300-nm sections. RR is a membrane-impermeant stain that binds only to membranes exposed to the external environment in nonpermeabilized cells (26). RR-stained vacuolar membranes were seen both near the surface and within the cell body (Fig. 1A and B), where they exhibited different levels of RR staining (Fig. 1A') (5, 28). Reconstructed tomograms obtained from serial sections were combined into large 3D images. Figure 1C to G show digital slices through such a 3D reconstruction. Previous 2D EM analyses of the HIV-1 macrophage assembly compartment suggested a con-

* Corresponding author. Mailing address: EMBL, Meyerhofstrasse 1, D-69117 Heidelberg, Germany. Phone: 49 6221 387 8192. Fax: 49 6221 387 8519. E-mail: welsch@embl.de.

▽ Published ahead of print on 25 May 2011.

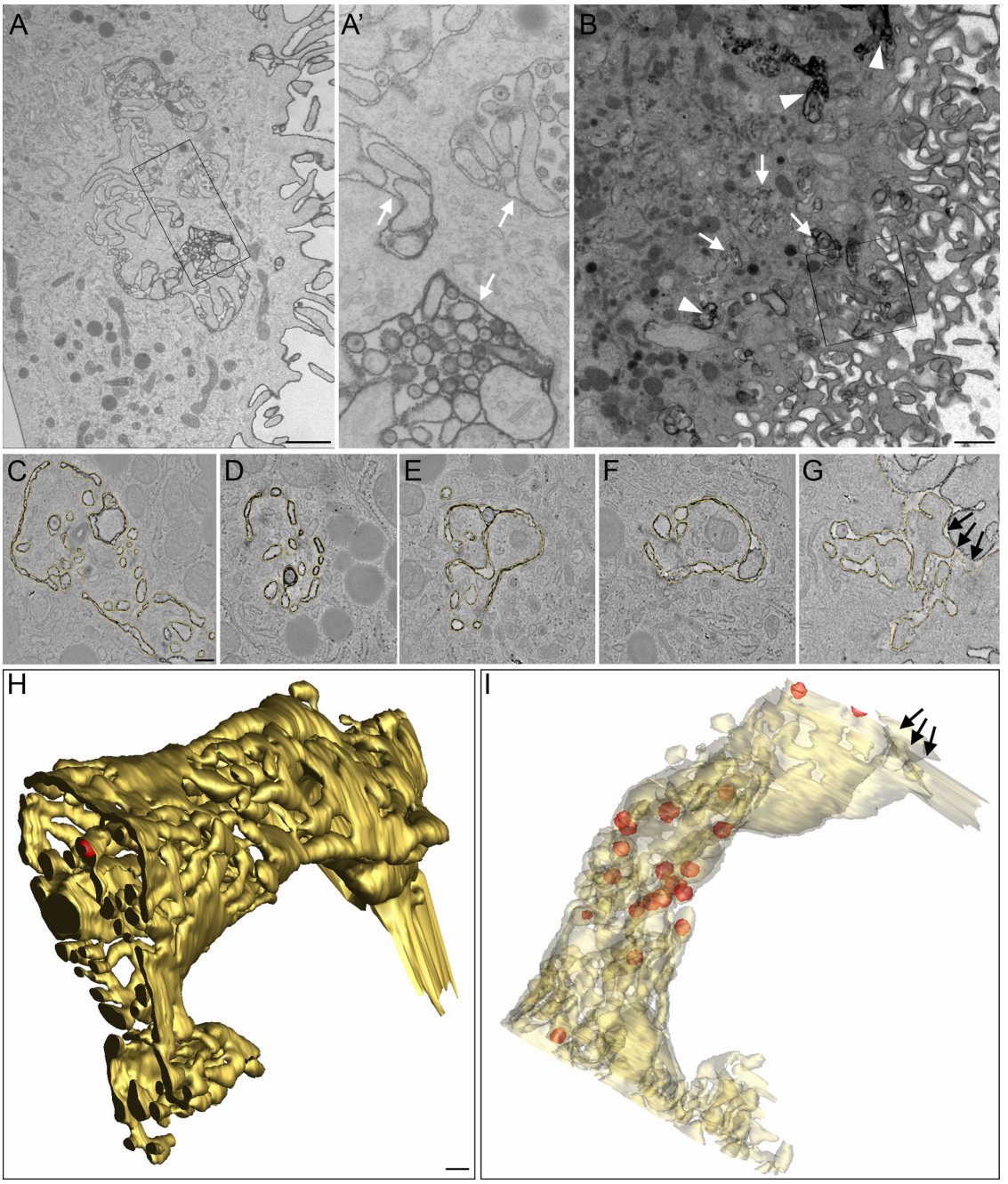

FIG. 1. Morphology of ruthenium red (RR)-stained membranes in macrophages and virus localization in the HIV-1 assembly compartment. (A) Thin section showing a cell profile sectioned perpendicularly to the cell substrate. The RR-stained plasma membrane has a complex morphology and forms virus-containing vacuolar structures inside the cytoplasm. (A') Higher magnification of the boxed area shown in panel A. Note that the level of RR staining varies between virus-containing vacuoles (white arrows). (B) Overview image of a 300-nm-thick macrophage section. This section is part of a section series that was used for the 3D reconstruction shown in panels C to I. The boxed area in panel B outlines the region used for reconstruction. Note that internal RR-stained compartments can appear very electron dense due to the close apposition and strong convolution of internal membranes (arrowheads) and that some virus-containing vacuoles are only partially stained or not RR stained (white arrows). (C to G) Digital slices through a tomogram showing the complex morphology of the RR-stained membrane (highlighted in yellow). The tubular exit site of the RR-stained compartment to the extracellular space is marked with arrows. (H and I) Two views of the surface-rendered RR-stained membrane compartment (yellow) and virus particles (red) in the tomogram outlined in panels C to G. In panel I, membranes are displayed semitransparently. The tubular exit site of the RR-stained compartment to the extracellular space is marked with arrows. Scale bar, 1 μm (A and B) and 200 nm (C to H).

voluted membrane morphology (5, 28), and our current analysis revealed a surprisingly complex and morphologically heterogeneous network of interconnected membranes. A 3D surface rendering of RR-stained membranes (Fig. 1H and I) visualized the complexity of such a membrane network (yellow), in which mature virus particles (red spheres) were found inside interconnected tubular-vacuolar structures of a membranous network. The membranes of this

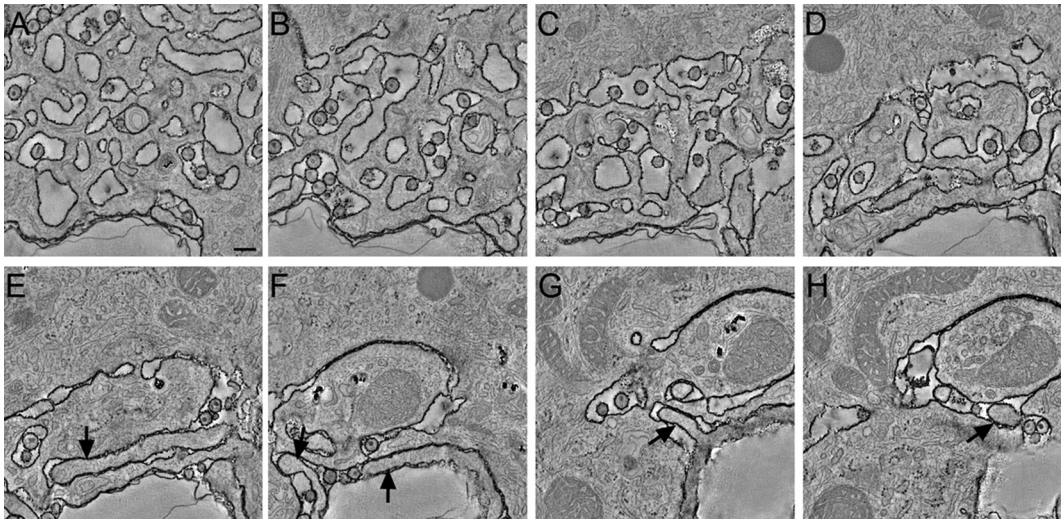

FIG. 2. Variable morphology of the HIV-1 assembly compartment. (A to H) Digital slices through a tomogram showing the variable morphology of the HIV-1-containing compartment. Depending on the size of vacuolar structures and the frequency of tubular connections and finger-like protrusions, different parts of the compartment appear as sponge-like structures (A to D) or as larger vacuoles containing finger-like protrusions (E to H, arrows). Scale bar, 200 nm.

labyrinth were highly convoluted, and thus the vacuoles often appeared to be interspersed by finger-like protrusions. There was no obvious preference for perinuclear or peripheral localization of virions. Virus budding structures were present but sparse (see Fig. 3B to D, arrowheads, and F, pink surfaces), precluding a detailed analysis of their distribution.

Depending on the size of individual vacuolar structures and the frequency of tubular connections, different parts of the same compartment appeared as either sponge-like structures (Fig. 2A to C) or as single, large vacuoles with or without filopodium-like protrusions (Fig. 2D to H). These morphologies have been described previously as different entities in 2D images of thin sections (5) but are now identified as elements of the same extensive network. We further investigated the connectivity of the compartment with the extracellular environment. Each compartment apparently had only one connection with the extracellular space (Fig. 1G and Fig. 3C, E, and F). The connection consisted of tightly apposed membranes and appeared as a bottleneck narrower than a virion diameter (Fig. 3C and F, arrows). Although our approach did not enable us to reconstruct images of entire cells, we nevertheless found that in each of the 3D images, RR-stained membranes could be traced as a single, continuous membrane. This result strongly suggests that each cell contains only one such continuous compartment. Thus, the individual HIV-1 storage compartments previously described in 2D thin sections of macrophages are interconnected and most likely surrounded by one continuous membrane, consistent with the results obtained by ion abrasion scanning electron microscopy (3).

Modulation of the virus-containing compartment upon infection. We wanted to determine whether the virus-containing compartment existed prior to infection, and if so, how extensive was the compartment and whether infection modulated its size and morphology. We used stereology, an approach that allows unbiased estimation of 3D surface area from 2D micrographs by estimating the boundary length of a structure and the area it covers (12). Macrophages from four different donors, each uninfected or infected with HIV-1, were stained with RR, fixed, embedded in a random orientation, and thin sectioned. Micrographs were acquired at predefined coordinates on thin sections, and the area and the boundary length of the RR-stained membrane compartment were estimated by systematic analysis of 50 images containing cell material for each sample. The described tubular compartment was observed in both uninfected and infected macrophages and thus apparently exists under physiological conditions and independent of HIV-1 infection. In uninfected macrophages, the membranous compartment covered on average ~1.5% of the total cell profile area (Fig. 4A, left panel). In infected cells, the membranous compartment increased to ~3.5%, demonstrating a significant ($P = 0.005$) virus-induced expansion. In most cell profiles, we also observed tubular-vacuolar structures that did not stain with RR and were of a morphology similar to that of RR-stained structures (Fig. 1A and B). These unstained structures covered a smaller area than the RR-stained compartment, also contained virions, and did not increase in size upon HIV-1 infection (Fig. 4A, right panel).

The total cell volume (including the RR-stained vacuole volume) of macrophages was estimated by the product of the area of macrophages on the cell culture dish (determined by light microscopy) and the average height of cells embedded perpendicular to the tissue culture dish (determined by EM). The average volume of macrophages from the three donors was not significantly affected by HIV-1 infection (Fig. 4B) ($P = 0.336$). Therefore, the expanded, internal RR-positive compartment is unlikely to be derived from *de novo*-synthesized membranes but rather is formed by invagination of preexisting plasma membrane or by fusion with cytoplasmic membrane organelles. The former would be predicted to lead to a decreased outer membrane surface area, a notion supported by the ratio of total RR-stained membrane length (outer plasma

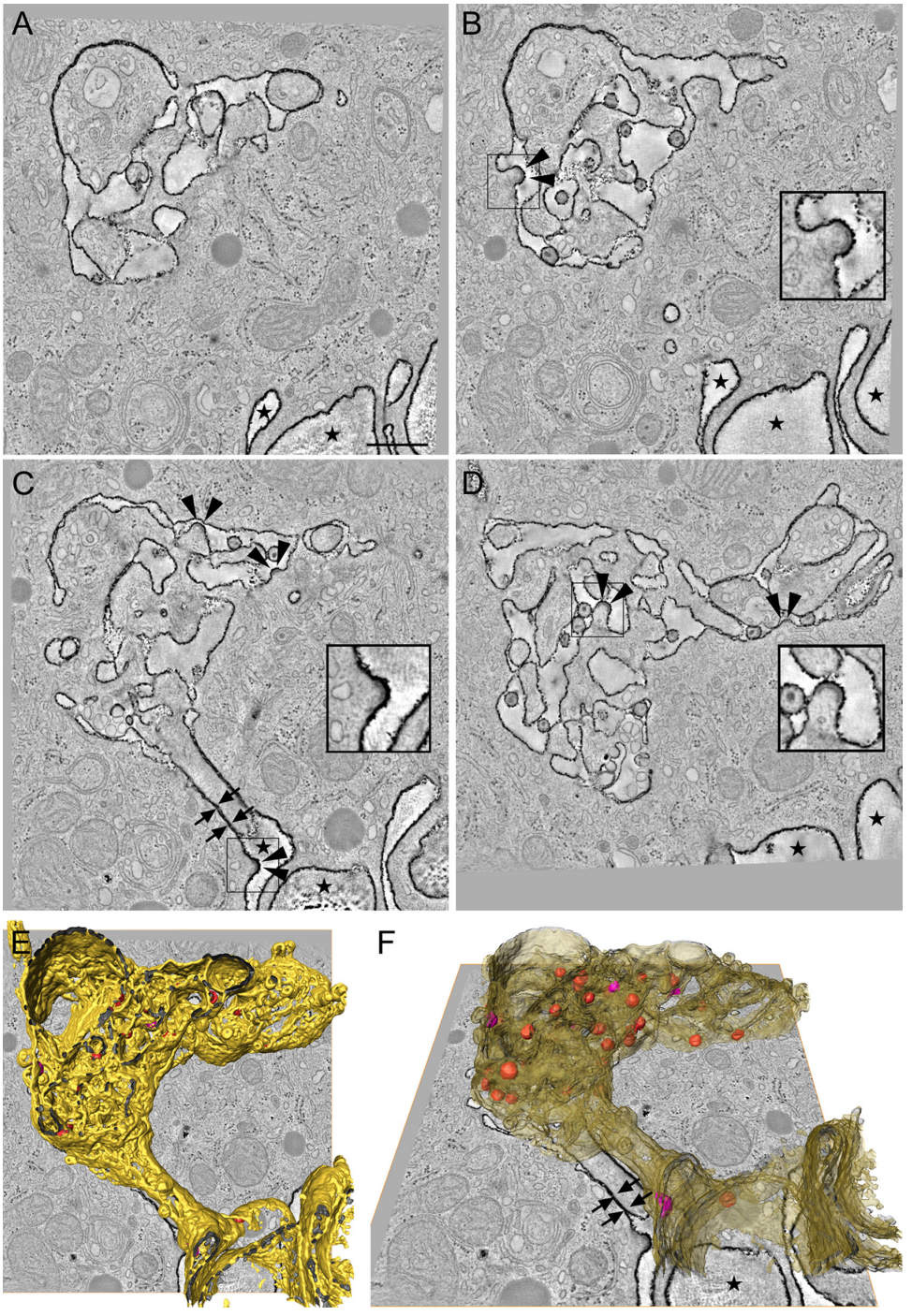

FIG. 3. Connectivity of the HIV-1 assembly compartment with the extracellular environment. (A to D) Digital slices of a tomogram showing the internal RR-stained, HIV-1-containing compartment connected to the extracellular space (marked with stars) via tightly apposed membranes that form a very narrow tube (C, arrows). Several HIV-1 budding structures are seen at the limiting RR-stained membrane of the compartment (B to D, arrowheads). Insets in panels B to D are higher-magnification views of virus budding structures in the boxed areas. (E and F) Two overlay views of a tomogram slice and the surface-rendered RR-stained membrane compartment (yellow, semitransparent in panel F), virus particles (red), and virus-budding structures (pink) in the tomogram outlined in panels A to D. Arrows indicate the tubular connection formed by two tightly apposed membranes; stars indicate extracellular space. Scale bar, 500 nm.

membrane and internally stained membrane) to internal RR-positive membrane length, which modestly decreased upon infection (Fig. 4C), although this trend did not reach a level of significance.

We also compared the membrane architectures of the outer cell surface and internal RR-stained structures by estimating the surface-to-volume ratios (surface densities) of macrophages and their internal RR-stained compartment. This re-

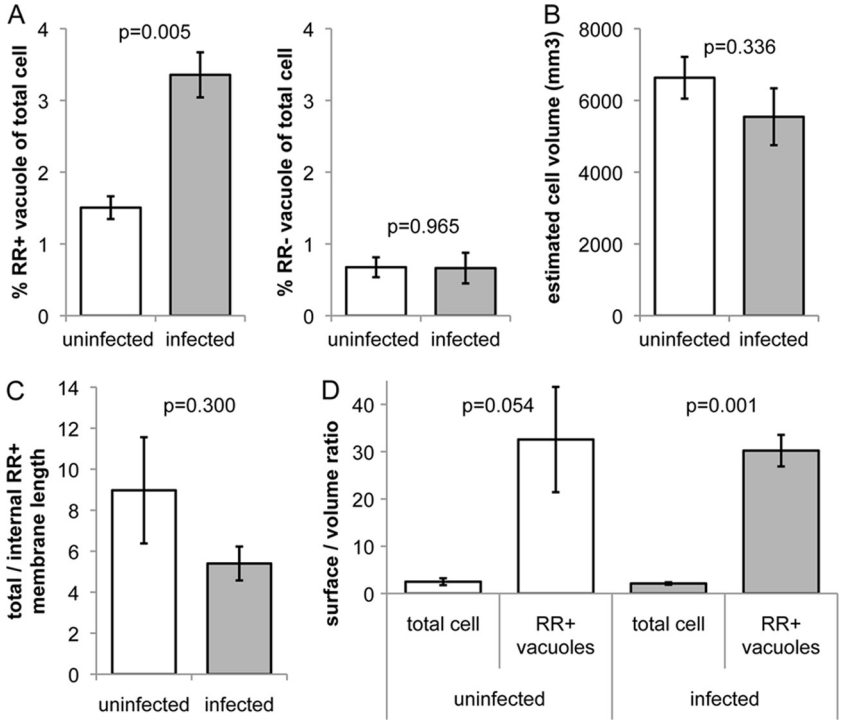

FIG. 4. Stereology analysis of membrane morphology in HIV-1-infected and uninfected macrophages. Cells were stained with RR, fixed, embedded in a random orientation, and thin sectioned. Micrographs were acquired at predefined coordinates (distance greater than an average cell profile) in at least two randomly chosen thin sections per sample and were systematically analyzed. (A) The cell profile area enclosed by RR-stained (RR+) membranes increases significantly upon infection (left panel, $P = 0.005$, two-tailed heteroscedastic Student's t test), whereas the area enclosed by RR-unstained (RR−) vacuolar membranes remains constant (right panel, $P = 0.965$). (B) The total cell volume of macrophages (including the RR+ vacuole volume) is not significantly decreased ($P = 0.336$) upon infection, indicating that the internal RR+ plasma membrane compartment is formed by invagination of the preexisting plasma membrane. (C) The ratio of total RR+ membrane length (outer plasma membrane and internal RR+ membrane) to internal RR+ membrane length decreases upon infection. (D) The surface-to-volume ratios (surface density) of total cells and the RR+ surface-accessible vacuolar structures significantly differ in both uninfected ($P = 0.054$) and infected ($P = 0.001$) cells. Data represent mean values derived from 50 images containing cell material from four (A) or three (B to D) independent donors, each uninfected or infected with HIV-1. Error bars, standard errors of the mean.

vealed that the surface density of the internal RR-positive tubular-vacuolar structures was significantly higher than that of the plasma membrane (Fig. 4D), indicating that internal membranes are highly convoluted. This is consistent with our tomographic analysis of the compartment that reveals a complex and extensive network of tubular membranes and suggests that folding and wrapping of plasma membrane sheets may contribute to formation of the internal compartment. HIV-1 infection did not substantially alter the surface densities of cells or the RR-positive compartment. This was expected, given that the surface density of cells and organelles is tightly regulated (20).

Our findings confirm recent studies demonstrating that HIV-1 accumulates in a surface-connected compartment within macrophages (3, 5, 28) and extend these studies by carrying out a detailed 3D morphological analysis of the macrophage compartment and revealing its expansion upon HIV-1 infection. The function and origin of the compartment in uninfected macrophages are unclear, but its morphology is consistent with older reports from ultrastructural studies in which surface-linked vesicular compartments were associated with the uptake and processing of horseradish peroxidase (22) and very-low-density lipoprotein (21). The surface-connected nature of the tubular structures is consistent with the near-neutral pH reported for the HIV-1 assembly compartment (15) and the lipoprotein uptake compartment (21). Clues may come from the work of Bennett et al. (3), who hypothesized that the compartment may be formed by the folding of large sheets of plasma membrane, trapping virus and other external structures within surface-connected tubular vesicles. If so, then this may be related to macropinocytosis, a nonspecific mechanism for antigen-presenting cells (APC) to sample the external milieu (6). However, it is clear from the presence of viral budding structures (28) that new HIV-1 virions are also produced and shed directly into this compartment. Therefore, formation of the tubular-vesicular structures by wrapping and folding of the plasma membrane may as well be induced upon HIV-1 infection even without macropinocytosis of virions. We therefore propose the term "HIV-1 assembly and holding compartment" to reflect both these potential functions. If the membrane sheets are dynamic and of a large surface area, this may help to explain why, in our snapshots of cell ultrastructure, we have observed only one distinct cell surface-connected compartment per cell. Large membrane sheets associated with virions have also been observed in HIV-1-pulsed dendritic cells (DC), suggesting that this may be a general feature of APC (8), although it should be noted that in this study the DC were not infected, and therefore only trapped virus was visualized.

We observed both RR-accessible structures close to the cell surface and RR-inaccessible membrane structures within the cell. This may reflect the diffusion limit to RR penetration into linked structures deeper within the cell or may indicate a distinct compartment that is not linked to the cell surface-connected compartment. At present, we are unable to determine which is more plausible, but surface-accessible tubular membrane structures have been observed to mature into closed lysosome-like compartments (21, 22), which may be an explanation. Previous studies have suggested that the difference in morphology between some relatively smooth virus-containing tubular vesicles and more-sponge-like complexes may represent distinct compartments (5, 15). Here we show that these structures are linked and appear to represent different morphological, and perhaps functional, states of the same compartment. Our stereology data show for the first time that the formation of the surface-connected tubular network is stimulated by HIV-1 infection. This suggests that productive infection of macrophages may activate pathways to increase membrane ruffling and macropinocytosis-like functions. Although we are not aware of previous studies demonstrating HIV-1 induction of such structures, HIV-1 infection has been shown to upregulate tunneling nanotubes in macrophages (7), a potentially related phenomenon.

In all the examples we have studied, the surface connection appeared thinner than the diameter of an HIV-1 particle. Although we cannot rule out minor membrane rearrangements upon chemical fixation, which might lead to changes in tubule diameter, our observations are in agreement with previous studies that such tubules are $<$100 nm (1, 3, 5, 22, 28). The diameter of the surface connections and the labyrinth-like nature of the compartment would limit diffusion of larger molecules and thereby may also aid in antibody evasion by HIV-1. It should be noted that the membranes of surface connections may be highly dynamic in living cells and thus the diameter of surface connections may rapidly change. Thus, the ability of HIV-1 to be rapidly transferred from infected macrophages to contacting $CD4^+$ T cells (11, 13) may result from collapse of the tubular compartment toward the point of T cell contact, allowing directed spread of virus to T cells across virological synapse-type structures. Future studies that analyze the accessibility of the compartment to particles of different sizes and the dynamic nature of the compartment during cell-cell contact are required to address these questions.

We thank C. Schwartz and the Boulder Laboratory for 3D Electron Microscopy of Cells in Boulder, CO, and W. Geerts and the 3D Electron Microscopy group, University of Utrecht, for advice and help with tomographic data collection and reconstruction. We also thank John A. G. Briggs and the European Molecular Biology Laboratory for substantial scientific and intellectual support. We are grateful to Anja Habermann and Ina Ambiel for technical support.

This work was supported in part by a grant from the Deutsche Forschungsgemeinschaft (SFB638) to H.-G.K., by The Wellcome Trust grant H5RCYV0 to Stephen D. Fuller, and by MRC grant G0901732 to Q.J.S. O.T.K. and H.-G.K. are investigators of the CellNetworks excellence cluster (EXC81). We thank Dormeur Investment Services Ltd. for support. Q.J.S. is a James Martin Senior Fellow.

REFERENCES

1. **Bainton, D. F., R. Takemura, P. E. Stenberg, and Z. Werb.** 1989. Rapid fragmentation and reorganization of Golgi membranes during frustrated phagocytosis of immobile immune complexes by macrophages. Am. J. Pathol. **134:**15–26.
2. **Benaroch, P., E. Billard, R. Gaudin, M. Schindler, and M. Jouve.** 2010. HIV-1 assembly in macrophages. Retrovirology **7:**29.
3. **Bennett, A., et al.** 2009. Ion-abrasion scanning electron microscopy reveals surface-connected tubular conduits in HIV-infected macrophages. PLoS Pathog. **5:**e1000591.
4. **Coleman, C. M., and L. Wu.** 2009. HIV interactions with monocytes and dendritic cells: viral latency and reservoirs. Retrovirology **6:**51.
5. **Deneka, M., A. Pelchen-Matthews, R. Byland, E. Ruiz-Mateos, and M. Marsh.** 2007. In macrophages, HIV-1 assembles into an intracellular plasma membrane domain containing the tetraspanins CD81, CD9, and CD53. J. Cell Biol. **177:**329–341.
6. **Doherty, G. J., and H. T. McMahon.** 2009. Mechanisms of endocytosis. Annu. Rev. Biochem. **78:**857–902.
7. **Eugenin, E. A., P. J. Gaskill, and J. W. Berman.** 2009. Tunneling nanotubes (TNT) are induced by HIV-infection of macrophages: a potential mechanism for intercellular HIV trafficking. Cell. Immunol. **254:**142–148.
8. **Felts, R., et al.** 2010. 3D visualization of HIV transfer at the virological synapse between dendritic cells and T cells. Proc. Natl. Acad. Sci. U. S. A. **107:**13336–13341.
9. **Finzi, A., A. Orthwein, J. Mercier, and E. A. Cohen.** 2007. Productive human immunodeficiency virus type 1 assembly takes place at the plasma membrane. J. Virol. **81:**7476–7490.
10. **Fischer-Smith, T., C. Bell, S. Croul, M. Lewis, and J. Rappaport.** 2008. Monocyte/macrophage trafficking in acquired immunodeficiency syndrome encephalitis: lessons from human and nonhuman primate studies. J. Neurovirol. **14:**318–326.
11. **Gousset, K., et al.** 2008. Real-time visualization of HIV-1 GAG trafficking in infected macrophages. PLoS Pathog. **4:**e1000015.
12. **Griffiths, G.** 1993. Chapter 11, Quantitative aspects of immunocytochemistry. Fine structure immunocytochemistry. Springer Verlag, Berlin, Germany.
13. **Groot, F., S. Welsch, and Q. J. Sattentau.** 2008. Efficient HIV-1 transmission from macrophages to T cells across transient virological synapses. Blood **111:**4660–4663.
14. **Joshi, A., S. D. Ablan, F. Soheilian, K. Nagashima, and E. O. Freed.** 2009. Evidence that productive human immunodeficiency virus type 1 assembly can occur in an intracellular compartment. J. Virol. **83:**5375–5387.
15. **Jouve, M., N. Sol-Foulon, S. Watson, O. Schwartz, and P. Benaroch.** 2007. HIV-1 buds and accumulates in "nonacidic" endosomes of macrophages. Cell Host Microbe **2:**85–95.
16. **Jouvenet, N., et al.** 2006. Plasma membrane is the site of productive HIV-1 particle assembly. PLoS Biol. **4:**e435.
17. **Kuroda, M. J.** 2010. Macrophages: do they impact AIDS progression more than CD4 T cells? J. Leukoc. Biol. **87:**569–573.
18. **Le Douce, V., G. Herbein, O. Rohr, and C. Schwartz.** 2010. Molecular mechanisms of HIV-1 persistence in the monocyte-macrophage lineage. Retrovirology **7:**32.
19. **Marsh, M., K. Theusner, and A. Pelchen-Matthews.** 2009. HIV assembly and budding in macrophages. Biochem. Soc. Trans. **37:**185–189.
20. **Morris, C. E., and U. Homann.** 2001. Cell surface area regulation and membrane tension. J. Membr. Biol. **179:**79–102.
21. **Myers, J. N., I. Tabas, N. L. Jones, and F. R. Maxfield.** 1993. Beta-very low density lipoprotein is sequestered in surface-connected tubules in mouse peritoneal macrophages. J. Cell Biol. **123:**1389–1402.
22. **Nichols, B. A.** 1982. Uptake and digestion of horseradish peroxidase in rabbit alveolar macrophages. Formation of a pathway connecting lysosomes to the cell surface. Lab Invest. **47:**235–246.
23. **Noursadeghi, M., D. R. Katz, and R. F. Miller.** 2006. HIV-1 infection of mononuclear phagocytic cells: the case for bacterial innate immune deficiency in AIDS. Lancet Infect. Dis. **6:**794–804.
24. **Pelchen-Matthews, A., B. Kramer, and M. Marsh.** 2003. Infectious HIV-1 assembles in late endosomes in primary macrophages. J. Cell Biol. **162:**443–455.
25. **Sattentau, Q.** 2008. Avoiding the void: cell-to-cell spread of human viruses. Nat. Rev. Microbiol. **6:**815–826.
26. **van Deurs, B., P. K. Holm, L. Kayser, and K. Sandvig.** 1995. Delivery to lysosomes in the human carcinoma cell line HEp-2 involves an actin filament-facilitated fusion between mature endosomes and preexisting lysosomes. Eur. J. Cell Biol. **66:**309–323.
27. **Venzke, S., and O. T. Keppler.** 2006. Role of macrophages in HIV infection and persistence. Expert Rev. Clin. Immunol. **2:**613–626.
28. **Welsch, S., et al.** 2007. HIV-1 buds predominantly at the plasma membrane of primary human macrophages. PLoS Pathog. **3:**e36.